Supporting Information

Unveiling the highly selective time-dependent colorimetric response of 8-hydroxyquinoline and indolinium-conjugated donor-π-acceptor (D-π-A) hybrid for the detection of copper(II) ions

G. Durga Prasad[a], Tadepalli Sanjeevakumar[a], Venkatachalam Rajeshkumar[b], Ashok K. Sundramoorthy[c] and Surendra H. Mahadevegowda[a,*]

[a]Department of Chemistry, School of Sciences, National Institute of Technology Andhra Pradesh, Tadepalligudem-534101, Andhra Pradesh, India.

[b]Organic Synthesis & Catalysis Lab, Department of Chemistry, National Institute of Technology Warangal, Hanumakonda –506004, Telangana, India.

[c]Centre for Nano-Biosensors, Department of Prosthodontics, Saveetha Dental College and Hospitals, Saveetha Institute of Medical and Technical Sciences, Poonamallee High Road, Velappanchavadi, Chennai, 600077, Tamil Nadu, India.

Email: surendra@nitandhra.ac.in

Table of Contents Page No.

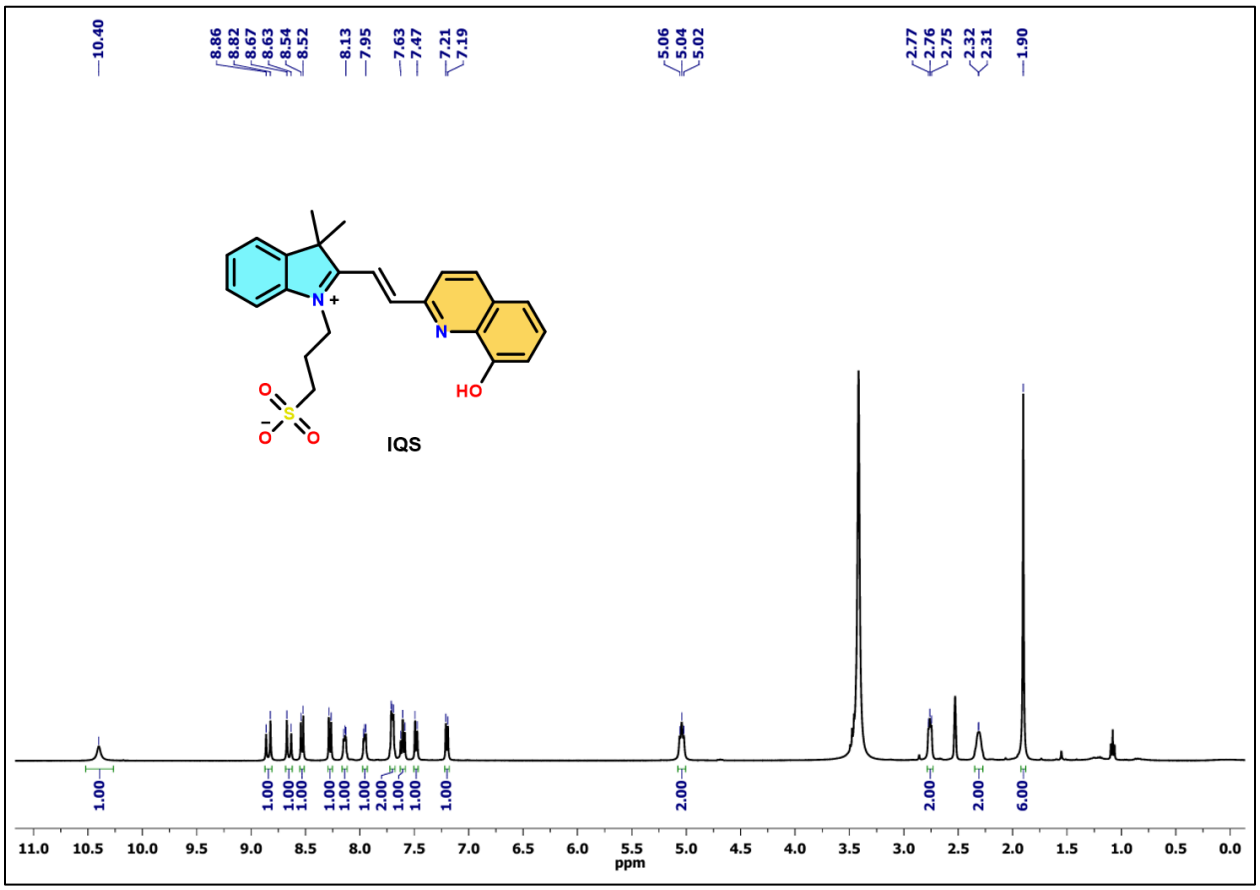

Fig. S1 ^{1}H-NMR Spectrum (400 MHz) of (E)-3-(2-(2-(8-hydroxyquinolin-2-yl) vinyl)-3,3-dimethyl-3H-indol-1-ium-1-yl) propane-1-sulfonate (**IQS**) in DMSO.

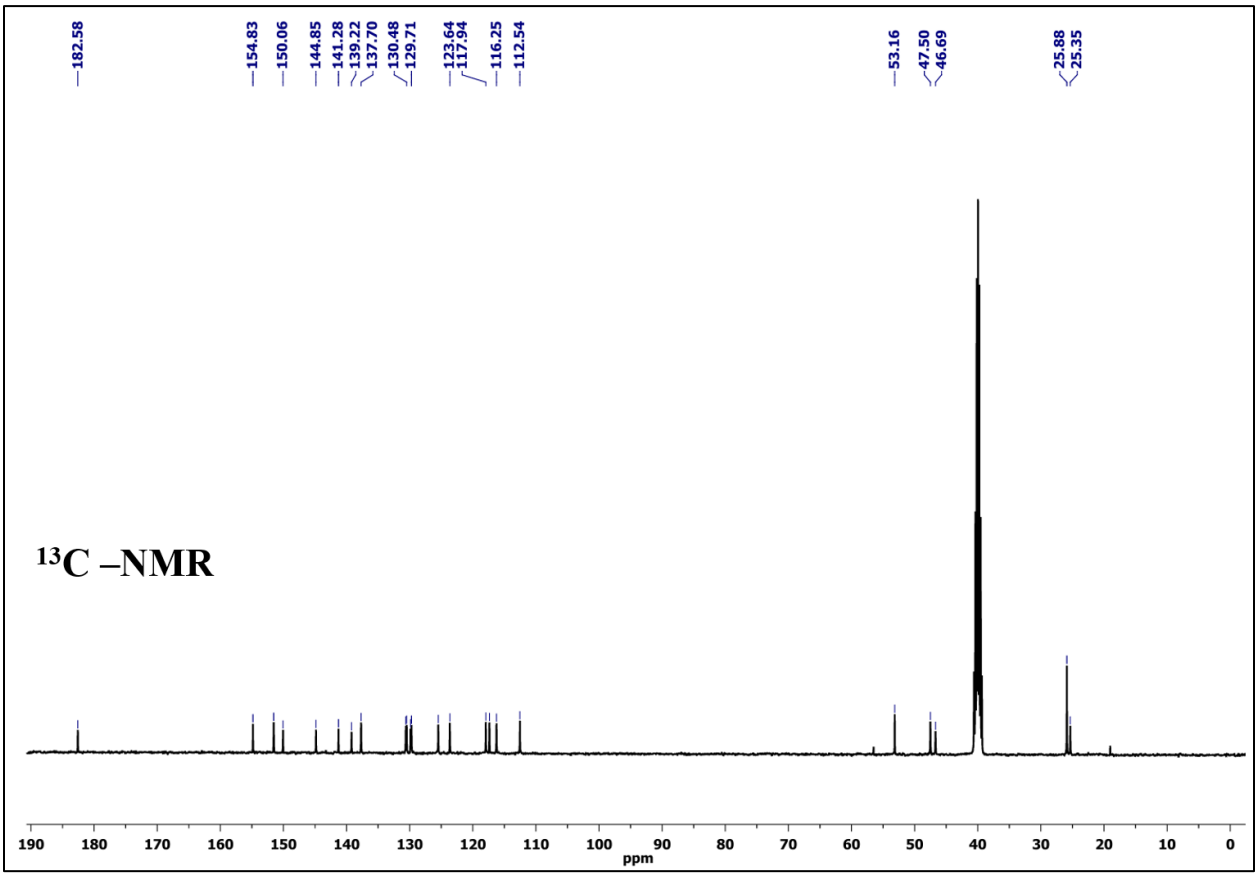

Fig. S2 ^{13}C-NMR Spectrum (100 MHz) of (E)-3-(2-(2-(8-hydroxyquinolin-2-yl) vinyl)-3,3-dimethyl-3H-indol-1-ium-1-yl) propane-1-sulfonate (**IQS**) in DMSO.

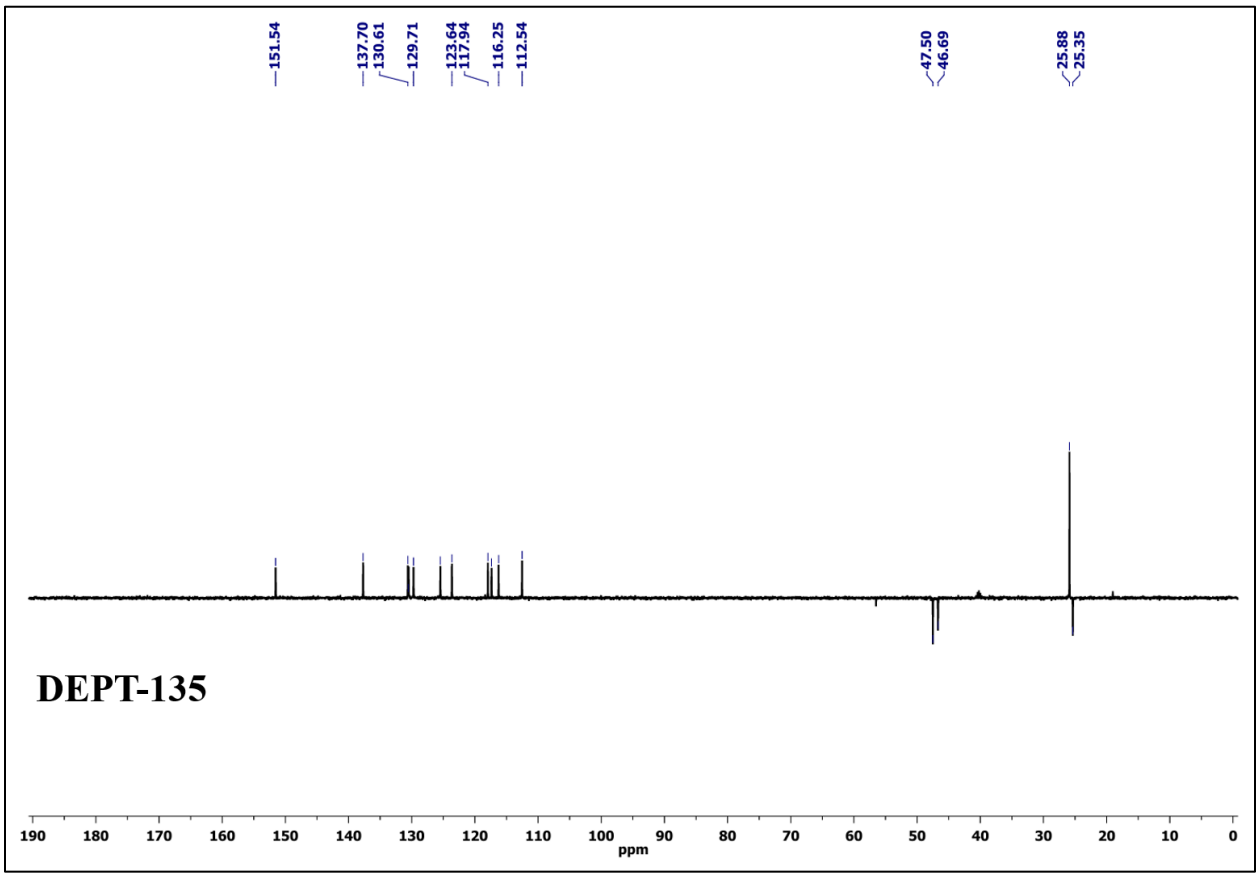

Fig. S3 DEPT-135 ^{13}C-NMR Spectrum (100 MHz) of (E)-3-(2-(2-(8-hydroxyquinolin-2-yl) vinyl)-3,3-dimethyl-3H-indol-1-ium-1-yl) propane-1-sulfonate (**IQS**) in DMSO.

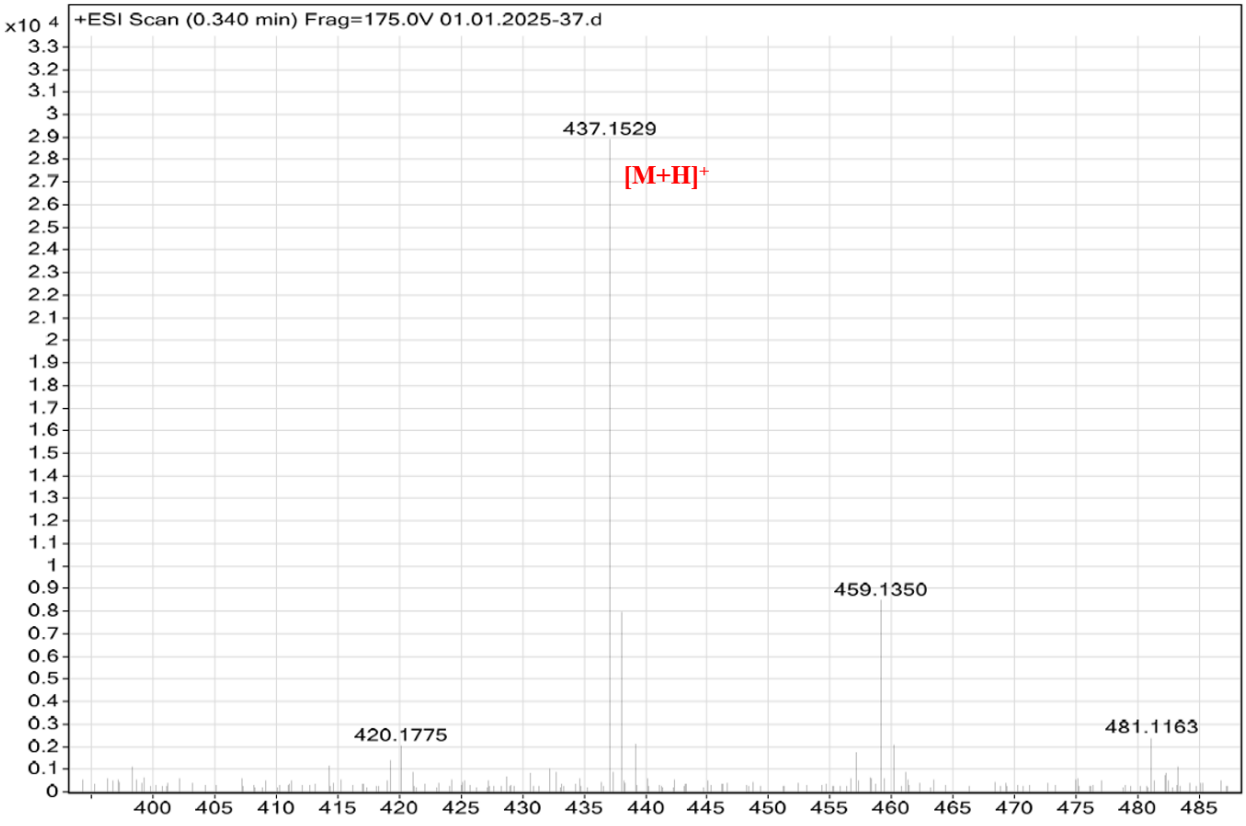

Fig. S4 ESI-MS Spectrum of (E)-3-(2-(2-(8-hydroxyquinolin-2-yl) vinyl)-3,3-dimethyl-3H-indol-1-ium-1-yl) propane-1-sulfonate (**IQS**). m/z calculated for $C_{24}H_{25}N_2O_4S$ $[M+H]^+$ **437.1530**; found **437.1529**.

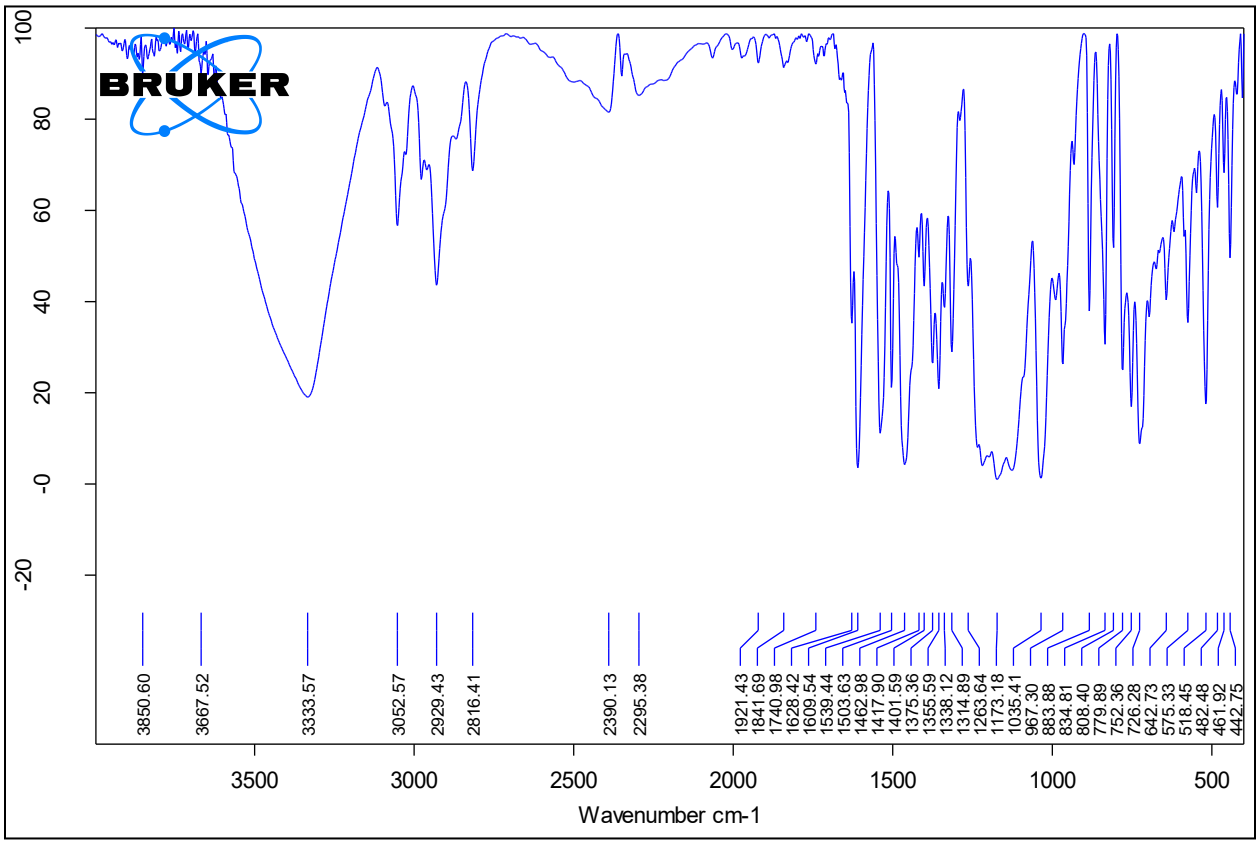

Fig. S5 FT-IR Spectrum of (E)-3-(2-(2-(8-hydroxyquinolin-2-yl) vinyl)-3,3-dimethyl-3H-indol-1-ium-1-yl) propane-1-sulfonate (**IQS**).

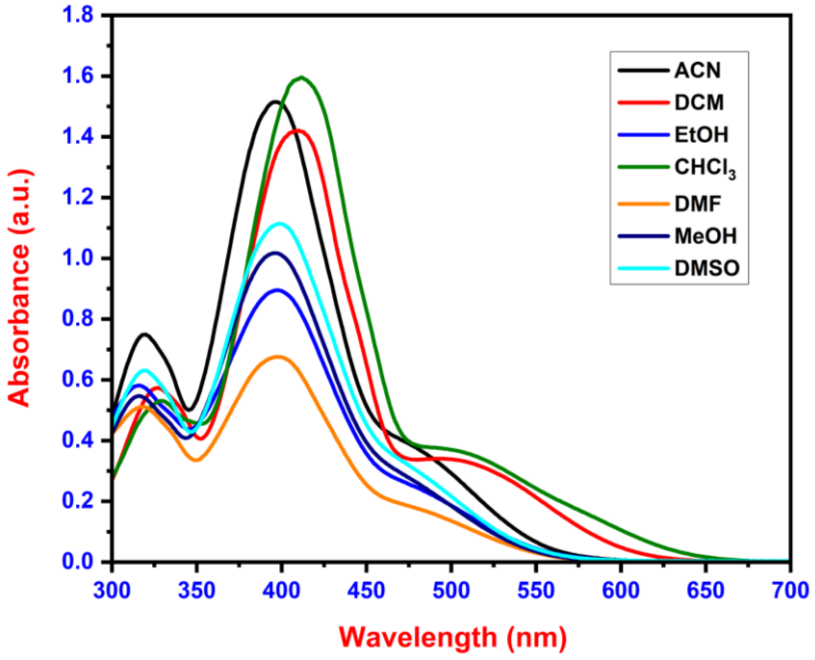

Fig. S6 Absorption spectrum of compound **IQS** (50 μM) in different solvents at room temperature.

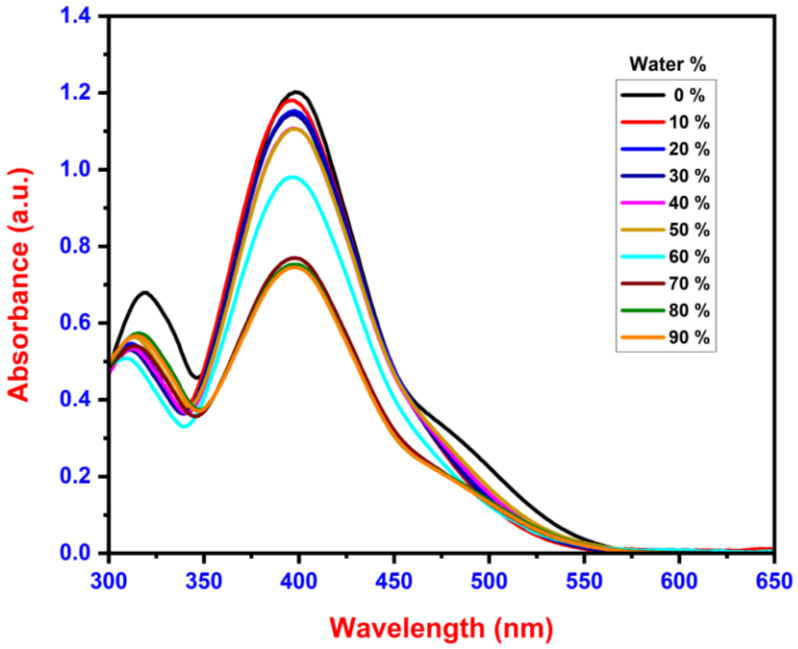

Fig. S7 Absorption spectrum of compound **IQS** (50 μM) in different water ratios in DMSO solvent at room temperature.

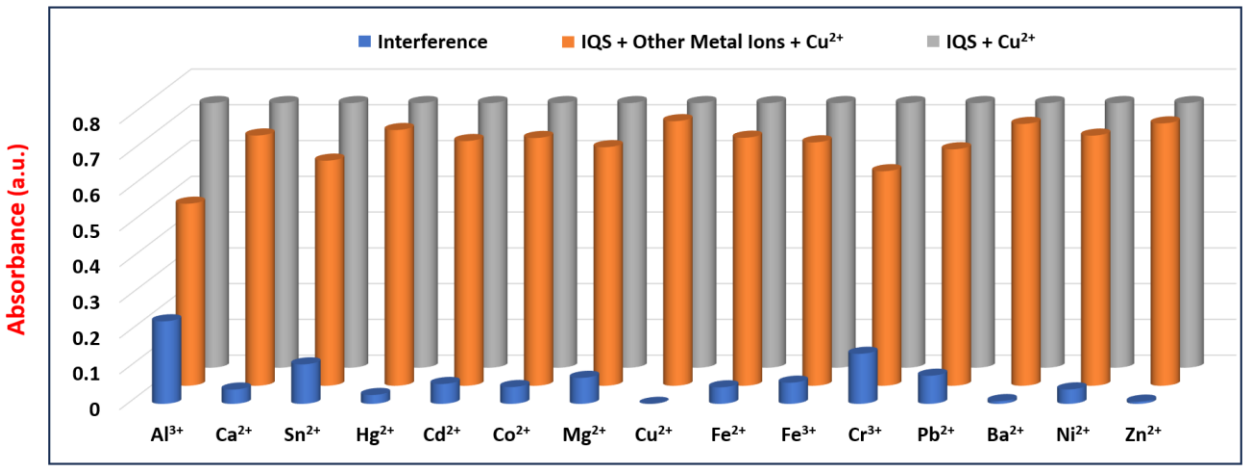

Fig. S8 Absorbance-mode interference analysis of **IQS** illustrating its selectivity toward Cu^{2+} in the presence of various competing metal ions (Recorded after 24 hours).

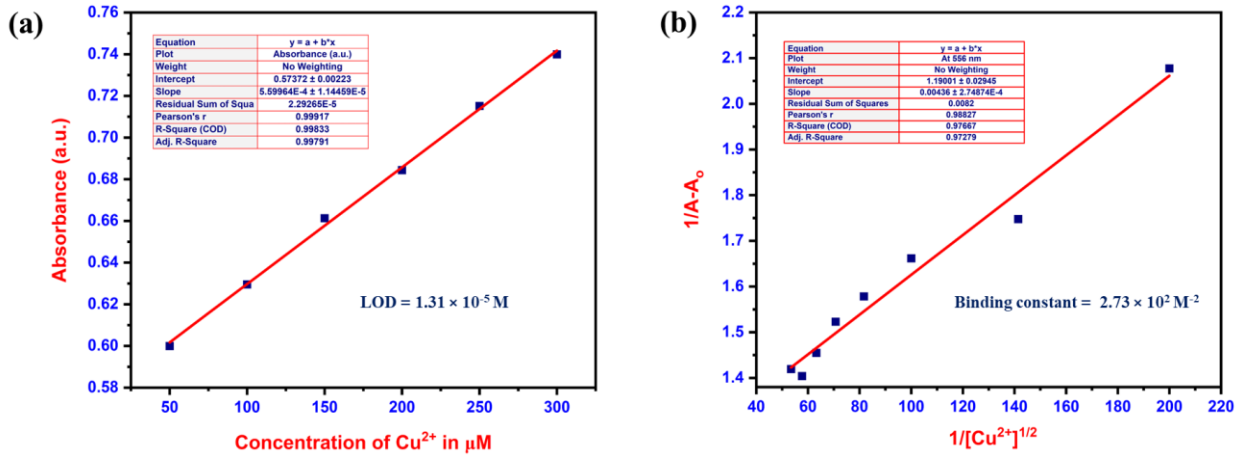

Fig. S9 (a) Variation of absorption intensity of **IQS** (50 µM) in DMSO-H_2O (8:2) solution with different concentrations of Cu^{2+} ions (50-300 µM) at 556 nm. (b) Benesi-Hildebrand plot for calculating the binding constant of the **IQS** with Cu^{2+} ions (Recorded after 24 hours).

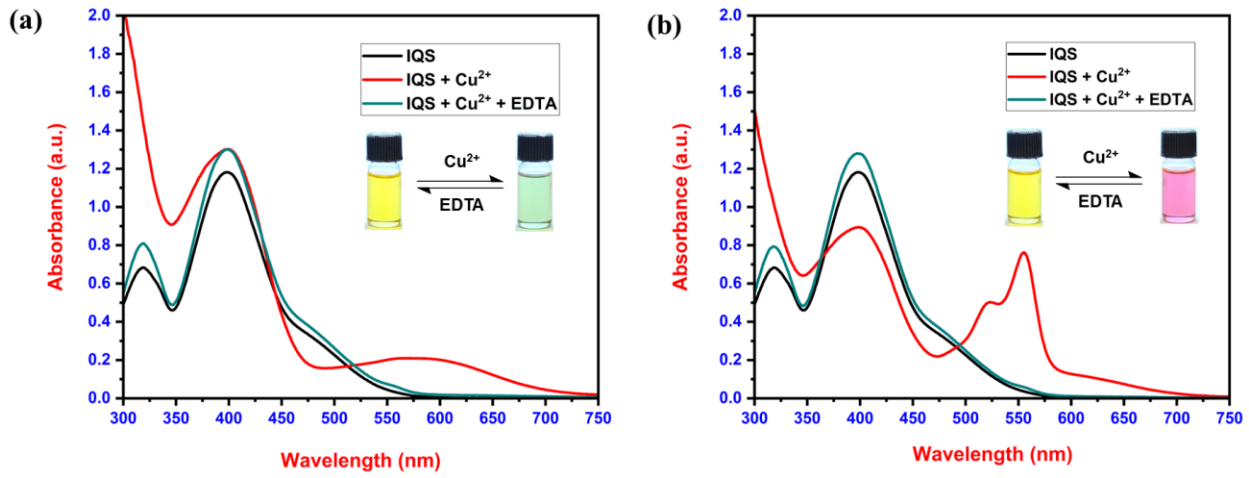

Fig. S10. (a) UV–Vis absorption spectra illustrating the reversible binding behavior of **IQS** toward Cu^{2+} within 5 minutes of addition. (b) UV–Vis absorption spectra showing the reversible interaction of **IQS** with Cu^{2+} after 24 hours, upon sequential addition of Cu^{2+} and EDTA.

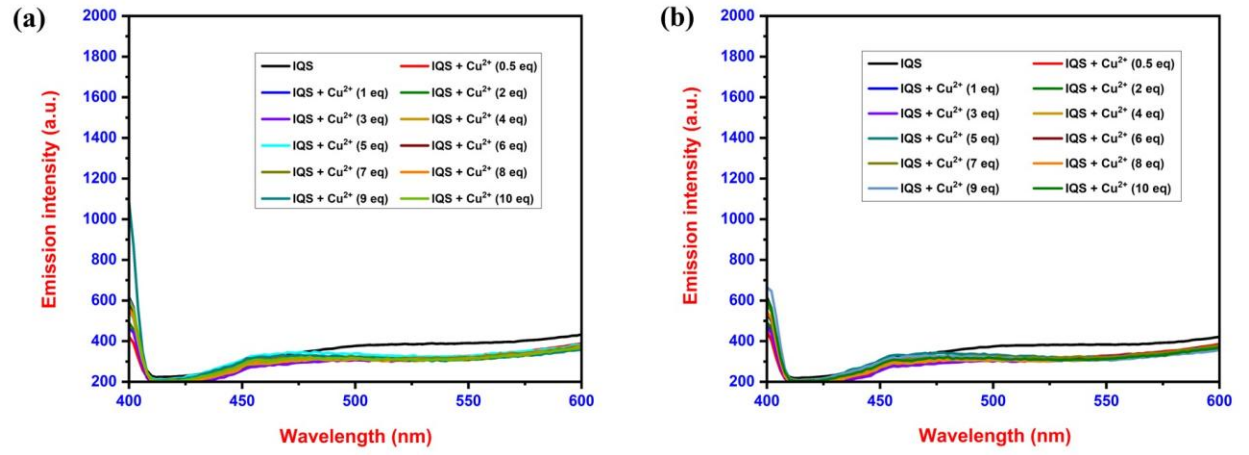

Fig. S11. Emission spectra of **IQS** (50 µM) in DMSO-H_2O (8:2) at room temperature are presented in (a) for incremental additions of Cu^{2+} ions (0-10 equivalents) and in (b) for the same system after 24 hours, together depicting the evolution of the **IQS-Cu^{2+}** spectral response over time.

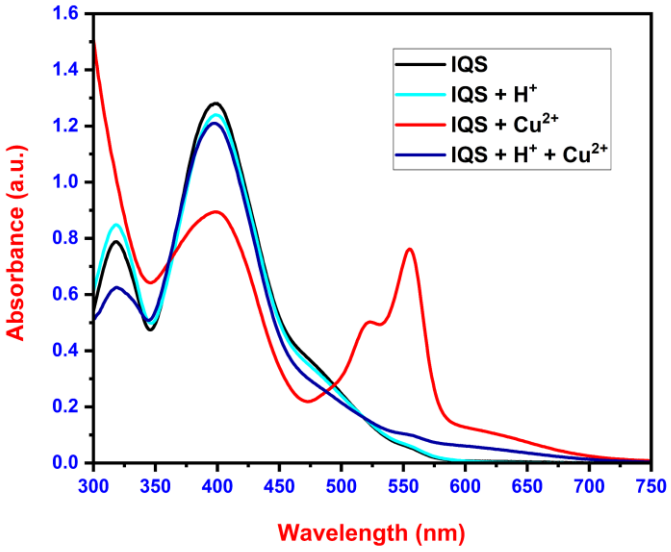

Fig. S12. UV–Vis absorption spectra of **IQS** alone and in the presence of H^+, Cu^{2+}, and both H^+ and Cu^{2+}, showing the influence of acidic conditions on Cu^{2+} binding and the spectral response of the probe.

Table. S1 Comparison of chemosensors for the recognition of Cu^{2+} ions reported in literature with the newly synthesized chemosensor **IQS** in the present work

S.No.	Chemosensor	Cu^{2+} (LOD)	Binding stoichiometric ratio	References
1	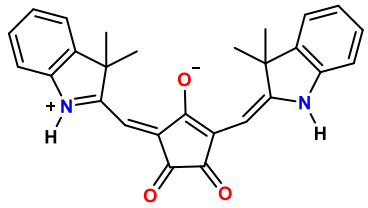	0.6×10^{-3} M	1:1	[1]
2	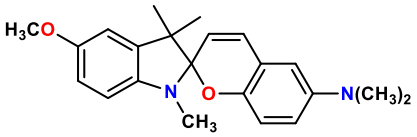	0.11×10^{-6} M	1:1	[2]
3	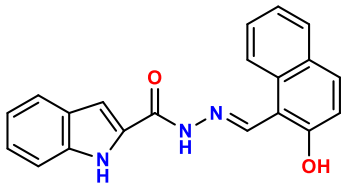	0.27×10^{-6} M	1:1	[3]
4	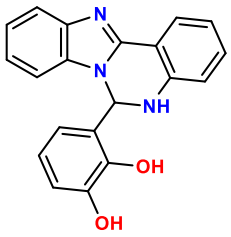	2.86×10^{-6} M	1:1	[4]
5	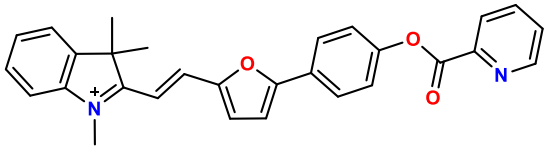	1.0×10^{-8} M	1:1	[5]

6	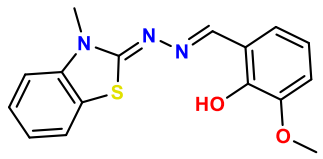	0.37 x 10^{-6} M	1:2	[6]
7	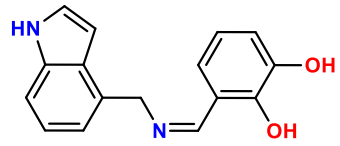	0.57 x 10^{-6} M	2:1	[7]
8	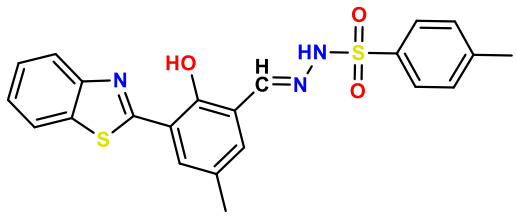	4.47 x 10^{-8} M	2:1	[8]
9	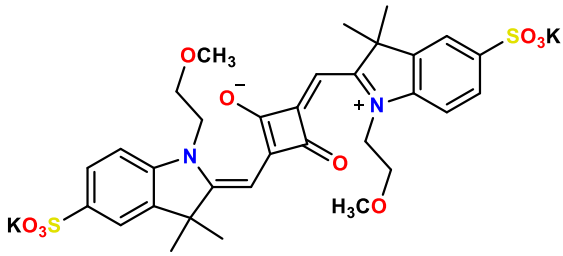	1.88 x 10^{-7} M	2:1	[9]
10	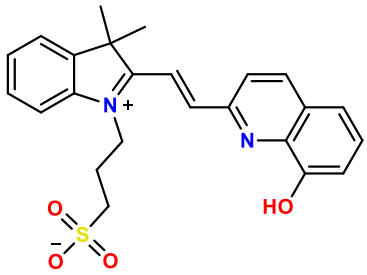	3.98 x 10^{-5} M (within 5 min) & 1.31 x 10^{-5} M (after 24 h)	2:1	Present work

Table. S2 Mulliken atomic charge distribution of **IQS** computed using DFT, B3LYP/6-311G(d,p) level of theory in DMSO.

Numbers	Atoms	Mulliken Atomic Charge	Numbers	Atoms	Mulliken Atomic Charge
1	C	0.251106	29	C	-0.06783
2	C	-0.04968	30	C	-0.09677
3	C	-0.06161	31	H	0.110121
4	C	-0.08927	32	H	0.124453
5	C	-0.10568	33	C	-0.09317
6	C	-0.05115	34	H	0.168482
7	C	0.37276	35	H	0.174696
8	H	0.120253	36	C	-0.21806
9	H	0.127223	37	H	0.143916
10	H	0.128469	38	H	0.146017
11	H	0.141303	39	C	-0.4215
12	C	-0.34734	40	H	0.165675
13	C	-0.20901	41	H	0.165431
14	H	0.134206	42	S	0.994004
15	H	0.139331	43	O	-0.62334
16	H	0.133918	44	O	-0.62901
17	C	-0.21846	45	O	-0.62896
18	H	0.14258	46	N	-0.43848
19	H	0.134195	47	C	-0.10575
20	H	0.137783	48	H	0.161269
21	C	0.101558	49	C	-0.03608
22	C	-0.09548	50	H	0.139269
23	C	0.03947	51	O	-0.36087
24	H	0.126891	52	H	0.282696
25	C	0.09421	53	N	-0.37157
26	C	-0.07843	54	C	-0.10964
27	H	0.120896	55	H	0.124107
28	C	0.160841			

Table. S3 Mulliken atomic charge distribution of **IQS+Cu^{2+}** complex computed using DFT, B3LYP/LanL2DZ level of theory in DMSO.

Numbers	Atoms	Mulliken Atomic Charge	Numbers	Atoms	Mulliken Atomic Charge
1	C	0.261717	56	C	0.305962
2	C	0.307404	57	C	-0.43611
3	C	-0.43727	58	C	-0.22912
4	C	-0.2308	59	C	-0.29161
5	C	-0.29074	60	C	-0.28018
6	C	-0.27973	61	C	0.319
7	C	0.313998	62	H	0.276216
8	H	0.27455	63	H	0.257688
9	H	0.257236	64	H	0.262037
10	H	0.262489	65	H	0.233139
11	H	0.256246	66	C	0.006745
12	C	-0.00506	67	C	-0.67479
13	C	-0.63259	68	H	0.222174
14	H	0.220066	69	H	0.233354
15	H	0.229639	70	H	0.233375
16	H	0.204785	71	C	-0.60937
17	C	-0.64611	72	H	0.243126
18	H	0.241665	73	H	0.231877
19	H	0.22987	74	H	0.216256
20	H	0.236478	75	C	0.05119
21	C	0.071659	76	C	-0.20988
22	C	-0.21198	77	C	-0.31116
23	C	-0.30921	78	H	0.236824
24	H	0.239909	79	C	-0.09681
25	C	-0.09745	80	C	0.373151
26	C	0.367589	81	H	0.280746
27	H	0.280323	82	C	0.180656
28	C	0.181066	83	C	-0.35528
29	C	-0.36059	84	C	-0.22489
30	C	-0.22251	85	H	0.267309
31	H	0.266868	86	H	0.260268
32	H	0.257744	87	C	-0.34027
33	C	-0.36623	88	H	0.213903

34	H	0.262248	89	H	0.298013
35	H	0.280476	90	C	-0.29913
36	C	-0.26672	91	H	0.209482
37	H	0.203659	92	H	0.260489
38	H	0.245561	93	C	-0.6471
39	C	-0.65111	94	H	0.297537
40	H	0.29422	95	H	0.274501
41	H	0.276452	96	S	1.182427
42	S	1.180429	97	O	-0.7219
43	O	-0.73786	98	O	-0.71147
44	O	-0.73826	99	O	-0.76198
45	O	-0.77681	100	N	-0.15937
46	N	-0.17828	101	C	-0.22531
47	C	-0.20715	102	H	0.259811
48	H	0.25771	103	C	-0.09297
49	C	-0.20169	104	H	0.223741
50	H	0.291403	105	N	-0.15255
51	N	-0.16825	106	C	-0.35013
52	C	-0.35719	107	H	0.27331
53	H	0.270695	108	O	-0.46333
54	Cu	0.473119	109	O	-0.44695
55	C	0.283655			

Table. S4. Calculated reactivity parameters of the probe **IQS** and its complexes with Cu^{2+} ions were computed using DFT at the B3LYP/6-311G(d,p) level for **IQS** and B3LYP/LanL2DZ for the metal complex with **IQS** in DMSO.

Parameters	**IQS**	**IQS+Cu^{2+}**
Electron affinity (EA)	3.386	4.091
Ionization potential (IP)	6.269	5.874
Chemical softness (σ)	0.694	1.121
Electronegativity (χ)	4.827	4.982
Chemical hardness (η)	1.441	0.891
Global softness (S)	0.347	0.561
Nucleophilicity index (N)	0.124	0.072
Chemical potential (μ)	-4.827	-4.982
Electrophilicity index (ω)	8.083	13.923
Electron-accepting capability (ω^+)	5.849	11.543
Electron-donating capability (ω^-)	10.677	21.092
Optical softness (σ_o) (eV^{-1})	0.346	0.561
Additional electronic charges (ΔN_{max})	3.348	5.588

Table. S5 The singlet excited-state properties of **IQS** and its complex with Cu^{2+} ions, including oscillator strengths and key electronic transitions, were computed using TD-DFT: B3LYP/6-311G (d, p) for **IQS** and B3LYP/LanL2DZ for the **IQS+Cu^{2+}** complex in DMSO.

	In DMSO solvent				
Compound	**Excited states**	**Excitation Energy (eV)**	**Excitation wavelength (nm)**	**Oscillator strength (f)**	**major transitions (% ge of contribution)**
IQS	1 (So → S_1)	2.295	540	0.000	H → L (99%)
	2 (So → S_2)	2.616	474	0.060	H-1 → L (99%)
	3 (So → S_3)	2.841	436	0.000	H-2 → L (99%)
	4 (So → S_4)	3.040	408	0.717	H-3 → L (94%)
	5 (So → S_5)	3.190	389	0.020	H-7 → L (93%)
	6 (So → S_6)	3.276	378	0.118	H-4 → L (86%)
	7 (So → S_7)	3.565	348	0.007	H-6 → L (56%)
	8 (So → S_8)	3.611	343	0.006	H-6 → L (40%), H-5 → L (58%),
	9 (So → S_9)	3.832	323	0.003	H-8 → L (99%)
	10 (So → S_{10})	4.167	297	0.036	H-9 → L (95%)

IQS+Cu^{2+}	1 (So → S_1)	0.359	3451	0.083	H → L (99%)
	2 (So → S_2)	0.677	1832	0.001	H-3 → L (86%)
	3 (So → S_3)	0.953	1301	0.022	H-6 → L (87%)
	4 (So → S_4)	1.056	1173	0.023	H → L+1 (99%)
	5 (So → S_5)	1.151	1077	0.003	H → L+2 (98%)
	6 (So → S_6)	1.381	898	0.000	H-1 → L (99%)
	7 (So → S_7)	1.454	852	0.002	H-11 → L (41%), H-10 → L (65%),
	8 (So → S_8)	1.504	824	0.004	H-12 → L (54%), H-9 → L (60%),
	9 (So → S_9)	1.523	814	0.001	H-11 → L (39%), H-9 → L (60%),
	10 (So → S_{10})	1.530	810	0.010	H-11 → L (77%)

References:

[1] S. Wang, Z. Li, S. Xu, C. Feng, An indolium croconine-based colorimetric and fluorescent chemosensor for detection Fe3+ and Cu2+, Optoelectronics and Advanced Materials-Rapid Communications 8(March-April 2014) (2014) 225-229.

[2] K.M. Trevino, B.K. Tautges, R. Kapre, F.C. Franco Jr, V.W. Or, E.I. Balmond, J.T. Shaw, J. Garcia, A.Y. Louie, Highly sensitive and selective spiropyran-based sensor for Copper (II) quantification, ACS omega 6(16) (2021) 10776-10789.

[3] Y. Singh, S. Arun, B.K. Singh, P.K. Dutta, T. Ghosh, Colorimetric and ON–OFF–ON fluorescent chemosensor for the sequential detection of Cu (II) and cysteine and its application in imaging of living cells, RSC Advances 6(83) (2016) 80268-80274.

[4] D. Wang, J.-Q. Zheng, X.-J. Zheng, D.-C. Fang, D.-Q. Yuan, L.-P. Jin, A fluorescent chemosensor for the sequential detection of copper (II) and histidine and its biological applications, Sensors and Actuators B: Chemical 228 (2016) 387-394.

[5] Y.-R. Wang, Y.-W. Tan, A.-H. Zhang, Y.-Y. Li, J.-L. Hu, J.-R. Wu, Z.-Q. Tian, Y.-F. Kang, The highly selective and sensitive fluorescence probe for detection of copper (II) ions and its bioimaging in vitro and vivo, Spectrochimica Acta Part A: Molecular and Biomolecular Spectroscopy 316 (2024) 124328.

[6] J.S. Heo, B. Suh, C. Kim, Selective detection of Cu2+ by benzothiazole-based colorimetric chemosensor: A DFT study, Journal of Chemical Sciences 134(2) (2022) 43.

[7] G.G.V. Kumar, P. Sharma, G. Thiruppathi, P. Sundararaj, A. Draksharapu, A highly selective indole-based sensor for Zn 2+, Cu 2+, and Al 3+ ions with multifunctional applications, Journal of Materials Chemistry B 13(25) (2025) 7335-7348.

[8] S. Zeng, S.-J. Li, X.-J. Sun, T.-T. Liu, Z.-Y. Xing, A dual-functional chemosensor for fluorescent on-off and ratiometric detection of Cu2+ and Hg2+ and its application in cell imaging, Dyes and Pigments 170 (2019) 107642.

[9] Y. Liu, L. Wang, C. Guo, Y. Hou, A colorimetric squaraine-based probe and test paper for rapid naked eyes detection of copper ion (II), Tetrahedron Letters 59(44) (2018) 3930-3933.

Gaussian 09, Revision A.02,

M. J. Frisch, G. W. Trucks, H. B. Schlegel, G. E. Scuseria, M. A. Robb, J. R. Cheeseman, G. Scalmani, V. Barone, B. Mennucci, G. A. Petersson, H. Nakatsuji, M. Caricato, X. Li, H. P. Hratchian, A. F. Izmaylov, J. Bloino, G. Zheng, J. L. Sonnenberg, M. Hada, M. Ehara, K. Toyota, R. Fukuda, J. Hasegawa, M. Ishida, T. Nakajima, Y. Honda, O. Kitao, H. Nakai, T. Vreven, J. A. Montgomery, Jr., J. E. Peralta, F. Ogliaro, M. Bearpark, J. J. Heyd, E. Brothers, K. N. Kudin, V. N. Staroverov, R. Kobayashi, J. Normand, K. Raghavachari, A. Rendell, J. C. Burant, S. S. Iyengar, J. Tomasi, M. Cossi, N. Rega, J. M. Millam, M. Klene, J. E. Knox, J. B. Cross, V. Bakken, C. Adamo, J. Jaramillo, R. Gomperts, R. E. Stratmann, O. Yazyev, A. J. Austin, R. Cammi, C. Pomelli, J. W. Ochterski, R. L. Martin, K. Morokuma, V. G. Zakrzewski, G. A. Voth, P. Salvador, J. J. Dannenberg, S. Dapprich, A. D. Daniels, O. Farkas, J. B. Foresman, J. V. Ortiz, J. Cioslowski, and D. J. Fox, Gaussian, Inc., Wallingford CT, 2009.